SMAR 2019 – Fifth Conference on Smart Monitoring,
Assessment and Rehabilitation of Civil Structures

SMAR 2019

Distributed Fiber Optics Monitoring of the Lago Bianco Dam in Switzerland

Tiziano CRAMERI [1], Alessio HÖTTGES [2], Carlo RABAIOTTI [2]
[1] Repower, Poschiavo, Switzerland
[2] HSR, Rapperswil, Switzerland

Contact e-mail: tiziano.crameri@repower.com

The Lago Bianco dam is a concrete gravity wall, which was built in 1911. The height of the dam was increased from 12 m to 16 m in 1942. Several conventional sensors accurately monitor the dam, including extensometers, piezometers, thermocouples, joint meters, GPS and geodetic instruments. Although the already existing sensors are adequate for monitoring the dam, an additional distributed fiber optics monitoring sensor system (DFOS) has been installed: The main goal was to verify the measurements of the conventional sensors, in particular strain, temperature and concrete crack development but with significantly higher spatial resolution. The DFOS were installed in a two dimensional grid on the downstream side of the dam and it was interrogated for more than four months on different time intervals. The DFOS enabled accurate and precise distributed measurements of the variation of temperature and strain of the dam surface. The collected data are in good agreement with the local measurements of the conventional sensors. Additionally, the DFOS allow for a more comprehensive understanding of the dam mechanical behaviour.

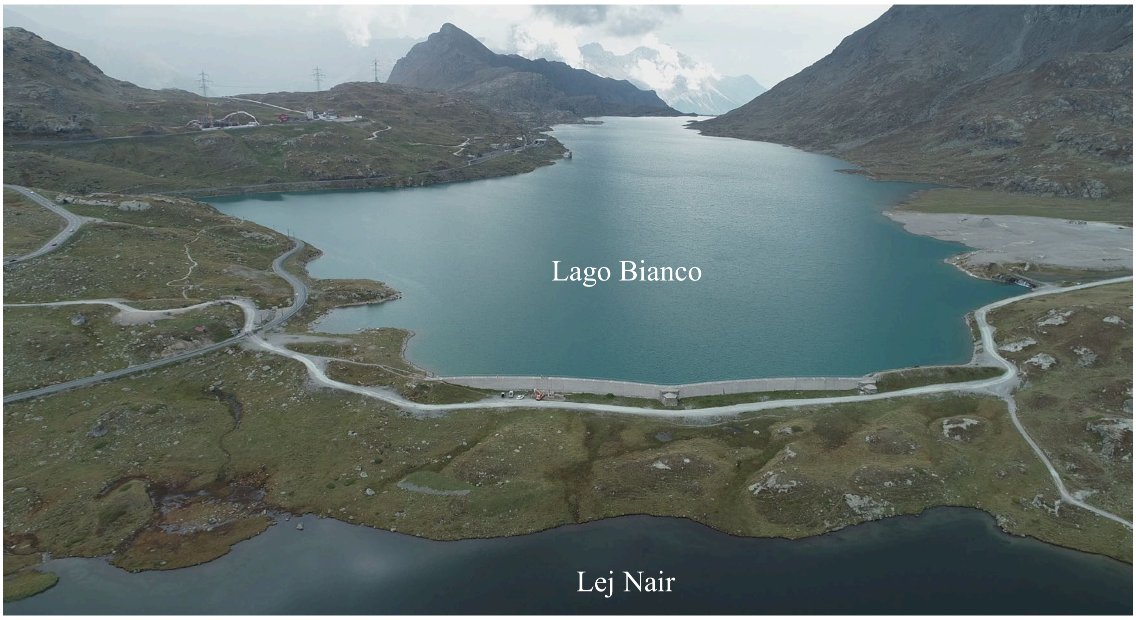

Figure 1. Lago Bianco Dam

1 INTRODUCTION

In recent years, the monitoring of structures has become increasingly important in the world of civil engineering. The economic and social repercussions of collapses or failures of structures go far beyond the investment to implement adequate monitoring systems. Furthermore, the existing structures are getting older and new ones are more and more sophisticated (Li, et al., 2004).

The use of fiber optics technology as a monitoring technique for measuring strains and temperatures has been developed in the early nineties (Horiguchi, et al., 1989).

An early application of this technology for dam monitoring was carried out by Glisic et al. in 1999 adopting SOFO fibre optics technology.

In the following years, this technology has developed reaching high accuracies and reliabilities. In general, three categories of fiber optic sensors are currently adopted: local (Fiber Bragg Grating: FBG), quasi-distributed and distributed fiber optic sensors (DFOS) (Villalba & Casas, 2013). The DFOS adopt for strain and temperature measurement the natural backscattering of the light within the glass fiber, for example, the Rayleigh, Brillouin or the Raman backscattered radiation. The core fiber itself acts as sensitive element (Hauswirth, 2015). The high-resolution distributed measurements deliver comprehensive information on the behaviour of the monitored structure (temperature and strain) with a single sensor and high spatial resolution (Inaudi & Glisic, 2005). In particular, when using the Swept-Wavelength Interferometry technique (SWI), it is possible to obtain a spatial resolution in the range of a few millimeters (Hauswirth, 2015). In case of concrete structures, this technology also enables the precise and accurate detection of the position and width of cracks (Villalba & Casas, 2013; Rabaiotti & Malecki, 2018).

The aim of this project is to analyse the adoption of DOFS based on SWI as a complementing monitoring system for an important Swiss dam, which belongs to the major electricity supplier REPOWER AG and is located in the beautiful scenery of the Bernina pass at Lago Bianco (Valposchiavo). The dam is subjected to considerable thermal gradients, which also according to literature, represent a major source of distress in dams exposed to very cold climates (Maken, et al., 2014). The results are successively compared with those obtained with the existing conventional monitoring system.

2 FIBER OPTIC SENSORS

Currently many different types of DFOS cables for measuring strains and temperatures are available. In this project, the BRUsens V9 and DTS are used. The BRUsens V9 is a strain sensor and is composed of a central fiber (single mode) glued to a metallic tube which is attached to an outer sheath to ensure the best strain transfer between concrete and core. The external layer is corrugated to enable perfect bond with the concrete. The BRUsens DTS is a temperature sensor. The DTS core fiber is not glued to the metallic tube but remains loose. Therefore, the induced strain is only due to temperature variations (Klar & Linker, 2010).

The adopted interrogator is the LUNA Optical Backscatter Reflectometer (OBR) 4600. The OBR 4600 is based on SWI technology. The measured spectral shift is directly proportional to a variation of strain and temperature.

3 TEST SITE AND INSTRUMENTATION

The northern dam of the Lago Bianco (2'235 m a.s.l.) is a gravity wall and consists of three interconnected arches with lengths of 75 m, 95 m, and 110 m respectively (Figure 1). The DFOS were installed on the centre part of the eastern arch in close proximity to the existing monitoring system, which includes two extensometers, one joint meter, one piezometer and five thermocouples inside the structure. The DFOS were fixed on the downstream side of the dam on a grid carved into the dam surface (see Figure 2).

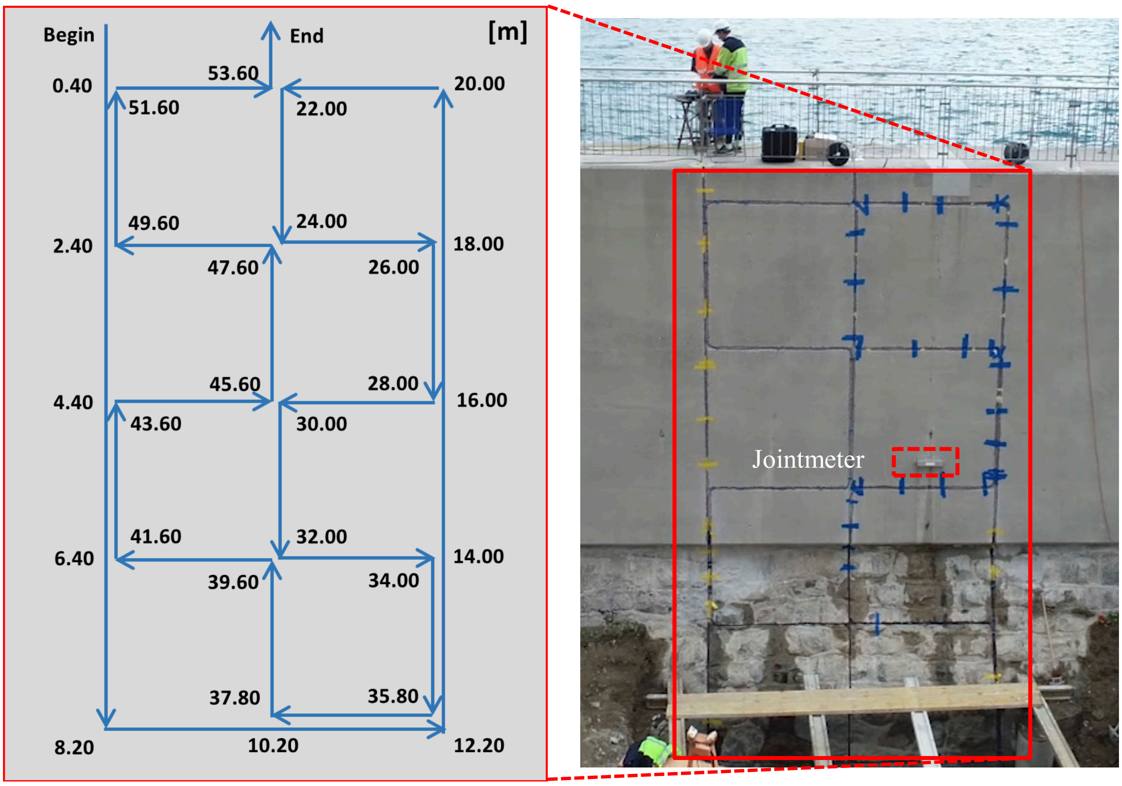

Figure 2. Path of the installed cable in the dam (left), position of the joint-meter (right)

The DOFS form a loop and the system was interrogated from both sides independently. Therefore, if the DFOS are damaged in one position, the whole cable length can still be interrogated. The interrogator has been positioned in a box with controlled and constant temperature conditions. After the installation of the cable, the trenches of the grid were filled with a high-strength mortar (usually adopted for dam repair) to avoid relative strain (displacement) between cables and concrete. The results presented in this paper range from September to December 2018. In this period of the year, the air temperatures decreased from +18 °C to -10 °C.

4 DATA ANALYSIS AND INTERPRETATION

4.1 Principles of the analysis

As mentioned before, the spectral shift $\Delta\nu_{OBR}$ between two measurements is directly proportional to the variation of the temperature ΔT and the strain $\Delta\varepsilon$. Mathematically this can be expressed by equation (1):

$$\Delta\nu_{OBR} = C_{\varepsilon,OBR} \cdot \Delta\varepsilon + C_{T,OBR} \cdot \Delta T \tag{1}$$

The proportionality coefficients $C_{\varepsilon,OBR}$ and $C_{T,OBR}$ are properties of each different fiber of the DFOS. The adopted cables V9 and the DTS share a similar fiber type, therefore we can assume that the coefficients are approximately equal. The strains and the temperatures can be obtained from equation (1), only if one of them is known. There are principally two different methods to obtain one of the two unknowns and to solve the equation (1): using two different fibers or using two different measurement techniques (Hauswirth, 2015). The simplest method is to measure with two independent DFOS, one of those only affected by temperature variation (like the DTS) and use this information to compensate the thermal effect on the second adjacent DFOS (V9). This procedure is carried out adopting equation (2), (Hauswirth, 2015).

$$\begin{cases} DTS\text{:} & \Delta\nu_{OBR,DTS} = C_{T,OBR,DTS} \cdot \Delta T \\ V9\text{:} & \Delta\nu_{OBR,V9} = C_{\varepsilon,OBR,V9} \cdot \Delta\varepsilon + C_{T,OBR,V9} \cdot \Delta T \end{cases} \Rightarrow \quad \Delta\varepsilon = \frac{\Delta\nu_{OBR,V9} - C_{T,OBR,V9} \cdot \frac{\Delta\nu_{OBR,DTS}}{C_{T,OBR,DTS}}}{C_{\varepsilon,OBR,V9}} \qquad (2)$$

4.2 Mapping of the cable

The initial and the end part of the grid were identified by heating the DFOS in different positions on the dam surface. This was necessary since the adopted interrogator OBR4600 start measuring the DFOS from the device. The heat source induced large strains in well determined positions of the DFOS allowing for a precise mapping of the signal on the installed grid.
Figure 2 represents schematically the installed grid. The grid geometry consists of eight adjacent rectangles and has total width of 4 m and a height of 7.80 m. The longest possible sensor length of 70 m dictates the dimensions of the grid. The embedded part of the DFOS has a total length of 54 m. The adopted geometry allows clearly separating between horizontal and vertical strain component variations.
The DFOS path was optimized in order to avoid crossings in the geometry, which could possibly disturb the embedment. Figure 2 (left) shows the geometry of the installed DOFS. The DFOS cross the main crack at three different levels therefore they monitor its evolution over the entire lenght. Information from a joint-meter is also available in one specific location. This allows comparing the measurements obtained with the DFOS with those from the joint-meter (Figure 2, right).

4.3 Measurement results

In general, it is important to remark that temperature and strain measurements obtained out with DFOS are only relative and not absolute and are always related to a reference zero measurement.

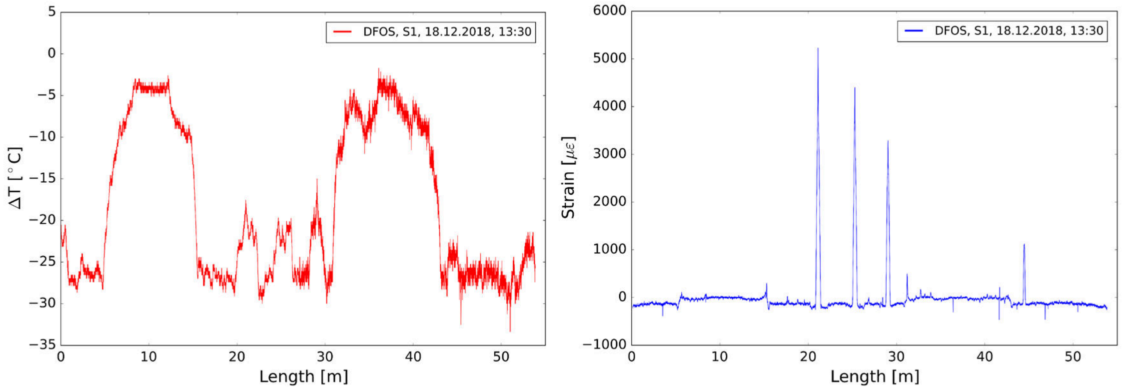

Figure 3. DFOS measured temperature (left) and strain (right) variation on the dam surface for the whole embedded sensor.

Figure 3 (left) shows the variation of temperature distribution (whole embedded sensor) on December 18th compared to the reference measurement on September 21st (first measurement).The measurements are plotted as if the sensor was "unrolled". The measurements reveal a remarkable temperature variation: the relative decrease in temperature is approximatively 25°C from September to December. Figure 3 (right) shows the variation of the strain measured on December 18th for the whole embedded DFOS. The measurement shows three to four main peaks (Figure 3 right) that correspond to the vertical crack intersections with the DFOS in three to four different positions.

Figure 4 illustrates superimposed the variations of the temperature and strain in different periods and positions on the dam surface. The temperature in the embedded part of the foundation is relatively stable; this is due to thermal insulation of the earth covering.

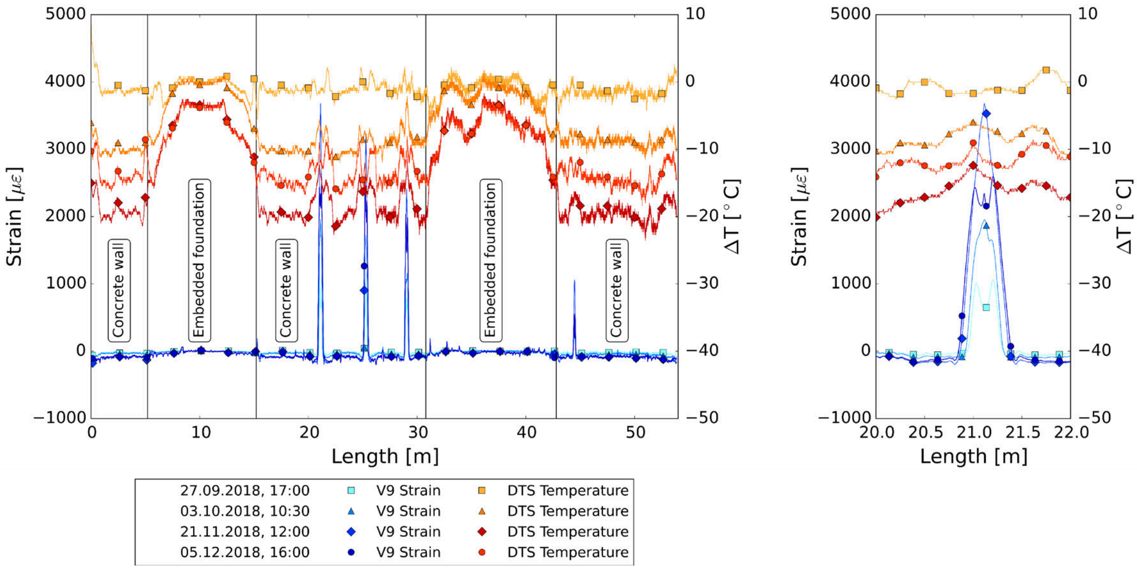

Figure 4. Superposition of temperature and strain measure for different periods. Right: detail of the crack

On the contrary, the portion of the DFOS installed in the concrete wall, directly exposed to air, shows a pronounced decreasing trend. Another important observation is that the strain peaks (clearly caused by the cracks) can also be identified in the DTS sensor cable in the same location (Figure 4). The fibers in the DTS sensor cables may begin to stretch as well when the cables undergo large deformations, thus becoming strain sensitive. This effect was already observed during preliminary laboratory tests as well as by other authors (Hauswirth, 2015). Nevertheless, this influence can be neglected for small strains as demonstrated by (Klar & Linker, 2010).

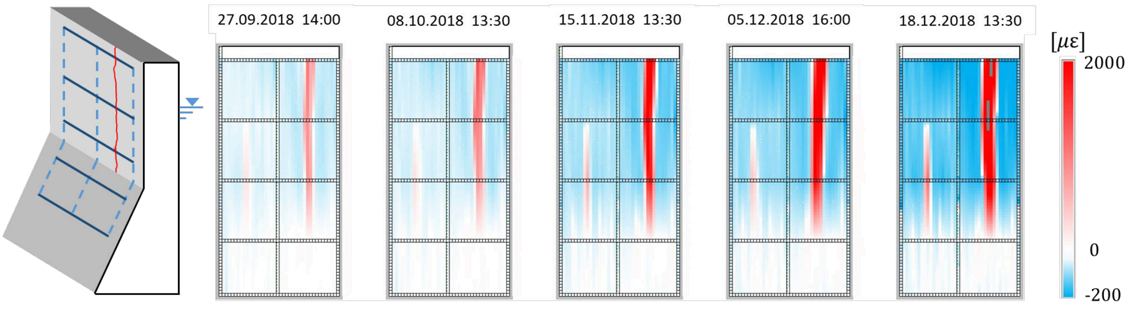

Figure 5. Horizontal strain field on the downstream face of the dam's wall

Figure 5 represents the evolution of the strain field along the dam's wall in different periods. The reference measurement was carried out the 21st of September.

The DFOS measurements are additionally linearly interpolated over the entire surface in order to obtain the two-dimensional strain field. The regions coloured blue correspond to compressive strain (negative) while the red ones represent tensile (positive) strain. The location of the vertical crack along the dam's wall, represented by the red coloured region, can clearly be observed. The visual inspection confirms the location of the crack in this position. The crack's strain peak increases during winter due to the decreasing temperatures, meaning that the crack is widening due to a shrinkage of the dam's wall. The temperature variation on the downstream surface of the wall is shown in figure 6. The reference zero measurement was taken the 21st of September.

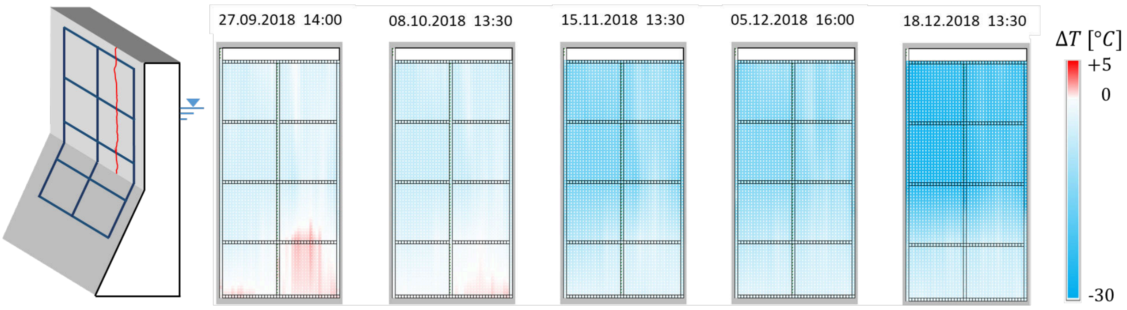

Figure 6. Temperature variation on the dam's downstream surface.

Figure 7 (left) shows the vertical extension/compression of the dam wall for three segments of the cable, each 4 m long (Figure 7, right). The results are obtained from the integration of the strains. It can be observed that:

- The compressive deformations increase with decreasing temperatures in winter
- In October measurements have been carried out with a regular schedule during the day. In this month the thermal gradient during the day is the highest. Based on these results, it can be concluded that the effect of temperature change during the day is neglectable

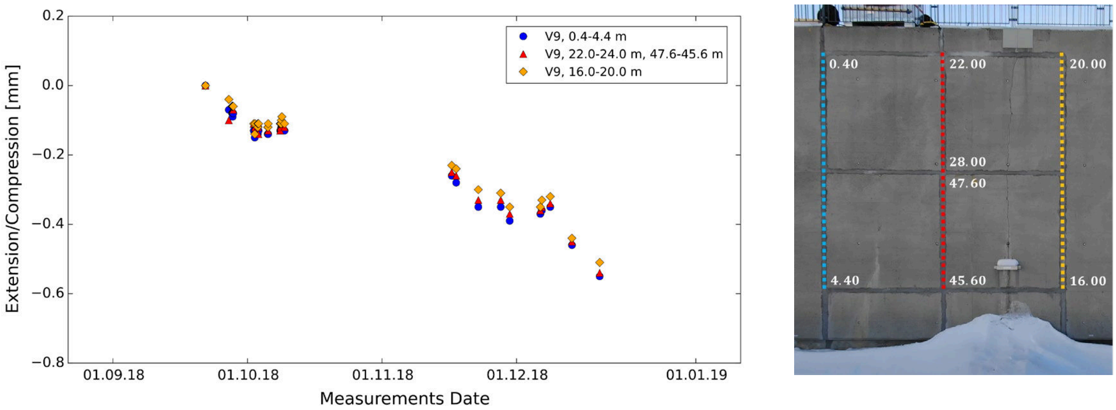

Figure 7: Vertical extension and compression of the dam wall (left), portion of the integrated cable (right)

5 COMPARISON WITH THE CONVENTIONAL MONITORING SYSTEM

The main vertical crack in the dam surface is monitored by a joint-meter. The effects of the crack are also clearly visible with the DFO strain sensor, where very large strains, higher than 2'000 microstrains, are measured (Figure 8, left). A simplified method is adopted in this paper to estimate the crack width from the DFOS measurement. In general the distance between the peaks in the strain measurement can be considered as the crack spacing. The crack width can be assessed integrating the tensile strain distribution on both sides of the peak (grey triangle in Figure 8, right). Obviously the crack width is much smaller than the region where tensile strains are measured: the cable is stretched in an area wider than the crack. This lead to the conclusion that the effects of the crack propagate for some cm in the mortar embedded part of the DFOS sensor cable.

On one hand, this prevents the DFOS from breaking, on the other the tensile strains are mainly due to the crack opening. Therefore, if the tensile strains are integrated over the representative length, the crack width can be obtained.

Figure 8 shows the crack openings measured with the joint-meter and with the DFOS for different periods. The trend of opening cracks with decreasing temperatures can clearly be observed. A very good agreement between the two measuring system is shown.

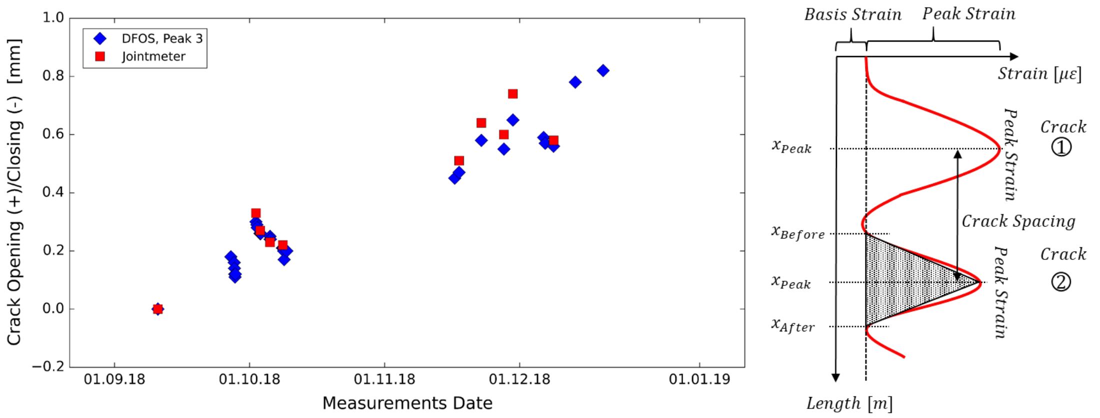

Figure 8: Comparison between the crack width from DFOS and the joint-meter (left), graphical representation of the crack's width calculation procedure (right)

6 INTEPRETATION OF THE RESULTS

The main goal of the DFOS system was to understand if the crack opening on the dam surface was only due to temperature or also from water loading and / or soil structure interaction problems. The measured vertical deformations are only due to negative thermal loading, since the water level from September to December did not change significantly (Figure 9).
The water temperature was always higher than 0°C, with a very low variation, therefore the thermal shrinking of the concrete took place mainly on the dam's downstream face, where the crack was developing. Additionally, the DFOS in the embedded part of the wall recorded very small dam deformations, where the temperature was more stable.

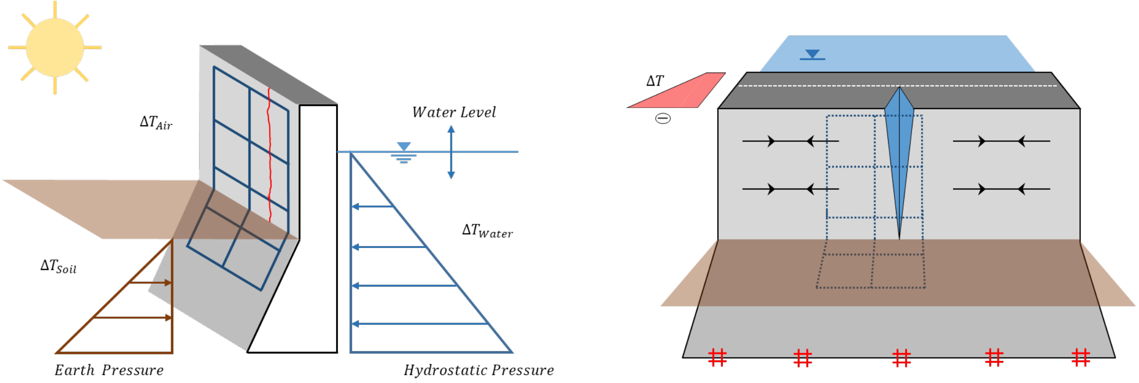

Figure 9: Loading conditions of the dam (left). Thermal distress of the dam (right)

7 SUMMARY AND CONCLUSIONS

DFOS interrogated with devices based on swept-length interferometry enable distributed measurements with high accuracy and precision, as well as extremely high spatial resolution. This is far beyond the results obtained with conventional monitoring systems.
The adoption of DFOS in this project lead to:

- A better understanding of the behaviour of the structure:The dam movement is mainly due temperature gradients rather than soil structure interaction and water loads

- The detection of the position and width of a crack, as well as its evolution over time
- A confirmation of the measurements from the conventional monitoring system

The results demonstrate that a large amount of conventional and different types of measuring devices (extensometers, temperature sensors, joint-meters) can be replaced by DFOS without losing any relevant information. On the contrary, the amount of information on a large spatial scale, which can be obtained with DFOS, cannot be obtained with any other conventional monitoring system.

The results from the DFOS can be now be used for the calibration of a three dimensional finite element model of the dam. This model will enable predicting the formation of cracks due to thermal shrinkage.

8 ACKNOWLEDGMENTS

The authors greatly acknowledge Dr. Dominik Hauswirth for his close support and highly competence advice.

9 REFERENCES

Bersan, S. et al., 2018. Distributed strain measurements in a cfa pile using high spatial resolution fibre optic sensors. *Engineering Structures,* Volume 160, pp. 554-565.

Glisic, B., Inaudi, D., Kronenberg, P. & Vurpillot, S., 1999. *Dam Monitoring Using Long SOFO Sensor.* Gmunden, Austria, Hydropower.

Hauswirth, D., 2015. *A Study of the Novel Approaches to Soil Displacement Monitoring Using Distributed Fiber Optic Strain Sensing.* Zürich: ETH Zürich.

Horiguchi, . T., Kurashima, T. & Tateda, M., 1989. Tensile strain dependence of Brillouin frequency shift in silica optical fibers. *IEEE Photonics Technology Letters,* 1(5), pp. 107-108.

Inaudi, D. & Glisic, B., 2005. Application of distributed Fiber Optic Sensory for SHM. *Proceeding of the ISHMII-2,* Volume 1, pp. 163-169.

Klar, A. & Linker, R., 2010. Feasibility study of automated detection of tunnel excavation by Brillouin optical time domain reflectometry. *Tunnelling and Underground Space Technology,* 25(5), pp. 575-586.

Li, H.-N., Li, D.-S. & Song, G.-B., 2004. Recent applications of fiber optic sensors to health monitoring in civil engineering. *Engineering structures,* 26(11), pp. 1647-1657.

Maken, D., Leger, P. & Roth, S., 2014. Seasonal Thermal Cracking of Concrete Dams in Northern Regions. *Journal of Performance of Constructed Facilities,* 28(4), pp. 1-14.

Rabaiotti, C. & Malecki, C., 2018. In situ testing of barrette foundations for a high retaining wall in molasse rock. *Geotechnique,* 68(12), pp. 1056-1070.

Smith, J., Brown, A., Demerchant, M. & Bao, X., 1999. Simultaneous distributed strain and temperature measurement. *Applied optics,* 38(25), pp. 5372-5377.

Villalba, S. & Casas, J. R., 2013. Application of optical fiber distributed sensing to health monitoring of concrete structures. *Mechanical Systems and Signal Processing,* 39(1-2), pp. 441-451.